*J. Fluid Mech.* (1996), *vol.* 326, *pp.* 37–56



# Miscible displacements in capillary tubes. Part 1. Experiments

By P. PETITJEANS[1,2] AND T. MAXWORTHY[1,3]

[1] Department of Aerospace Engineering, University of Southern California, Los Angeles, CA 90090-1191, USA

[2] Laboratoire de Physique et Mecanique des Milieux Heterogenes, Ecole Superieure de Physique et Chimie Industrielles, 10, Rue Vauquelin, F-75231, Paris cedex 05, France

[3] Department of Mechanical Engineering, University of Southern California, Los Angeles, CA 90089, USA

(Received 11 January 1996 and in revised form 6 May 1996)

Experiments have been performed, in capillary tubes, on the displacement of a viscous fluid (glycerine) by a less viscous one (a glycerine–water mixture) with which it is miscible in all proportions. A diagnostic measure of the amount of viscous fluid left behind on the tube wall has been found, for both vertical and horizontal tubes, as a function of the Péclet (*Pe*) and Atwood (*At*) numbers, as well as a parameter that is a measure of the relative importance of viscous and gravitational effects. The asymptotic value of this diagnostic quantity, for large *Pe* and an *At* of unity, has been found to agree with that found in immiscible displacements, while the agreement with the numerical results of Part 2 (Chen & Meiburg 1966), over the whole range of *At*, is very good. At values of the average *Pe* greater than 1000 a sharp interface existed so that it was possible to make direct comparisons between the present results and a prior experiment with immiscible fluids, in particular an effective surface tension at the diffusing interface could be evaluated. The effect of gravity on the amount of viscous fluid left on the tube wall has been investigated also, and compared with the results of Part 2. A subsidiary experiment has been performed to measure both the average value of the diffusion coefficient between pure glycerine and several glycerine–water mixtures, in order to be able to calculate a representative Péclet number for each experiment, and the local value as a function of the local concentration of glycerine, in the dilute limit.

## 1. Introduction

An improved understanding of the dynamics of multiphase porous media flows remains an essential prerequisite for progress in the fields of enhanced oil recovery, fixed bed regeneration, hydrology, and filtration. From basic stability theory (Chouke, van Meurs & van der Pol 1959; Saffman & Taylor 1958) we know that if the displacing fluid is less viscous than the displaced fluid, the unfavourable mobility profile will lead to the well-known fingering instability, which causes the displacing fluid to channel through the displaced zone, thereby reducing the efficiency of the displacement process. If the fluids are of different densities, gravity can exert an additional stabilizing or destabilizing influence. Reviews on this topic are given by Homsy (1987), Saffman (1986) and Bensimon *et al.* (1986). Depending on whether the two fluids are *immiscible* or *miscible*, one can distinguish two apparently different problems. In the immiscible case, where the surface tension acts at the interface between the two fluids, the capillary

number, which is a measure of the ratio of viscous to surface tension forces, represents a dynamically important parameter. It determines the most unstable wavelength of the fingering instability as well as the dynamics of the evolving fingers, e.g. Maxworthy (1989), Meiburg & Homsy (1988).

For miscible displacements, however, it is conventionally assumed that the dynamics are determined by the relative importance of convective and diffusive effects but, in general, the proper form of the diffusion tensor to be used within the mixing region in theoretical/analytical studies is not known. Past investigations have employed rather *ad hoc* approaches that have been developed without the advantage of comparison with rigorous, experimental or numerical studies. The simplest assumption, that of isotropic diffusion of the two phases, certainly cannot describe the reality of flow in a porous medium nor in a depth-averaged Hele-Shaw flow. Tan & Homsy (1986), Yortsos & Zeybek (1988), Brady & Koch (1988) as well as Zimmermann & Homsy (1991) have taken the first steps towards a more realistic approach by assuming a variety of conditions based on various forms of the diffusion tensor at the interface, e.g. isotropic or anisotropic diffusion that may or may not depend on the velocity field there. In the stability analyses it is assumed that the basic density and viscosity profiles change more slowly than the rate at which the instability grows, and all give growth rates and interface shapes that can, in principle, be checked against experiments. Another approach to the stability problem based on the idea of an effective surface tension has been presented by Hu & Joseph (1991), also under the rather restrictive assumption that the species concentration can be averaged over the cross-section of the gap. Further, Joseph (1990) has considered a number of experiments in which a bubble or drop of one fluid moved through another fluid with which it was miscible in all proportions. We note for future reference that such observations cannot represent a steady-state situation since interior fluid is continually being removed at the interface and deposited into a wake. Joseph made the interesting point that the form of these bubbles is similar to those found in immiscible fluids with a large surface tension. While it is possible to make such qualitative comparisons very easily it is far harder to make them quantitative in such a complex free-boundary flow with many parameters. In the present work a simpler geometry is considered from which quantitative results can be obtained. Also, in his recent work, Joseph pointed out that in the diffusion region between two incompressible flows, the assumption of a divergence-free mass-averaged velocity fields may not always be a good approximation, even if the volumes of the fluids so not change. Consequently, this effect plus additional stress terms (the so-called Korteweg stresses (Korteweg 1901)) might play a role in the diffusing region, which can mimic the effect of an interfacial tension even in miscible displacement processes. Values of 'effective' surface tension, $\sigma_{eff}$, in the range of 1 to $10^{-4}$ dyn cm$^{-1}$ have been suggested.

In the present work in order to simplify the interpretation of the experiments we have considered mainly flow in basic geometries, e.g. those between closely spaced parallel plates (a Hele-Shaw cell) or within capillary tubes. The former is usually considered as a limiting model for two-dimensional motion in an extended porous medium (e.g. Homsy 1987), while the latter could be considered as the simplest model of displacement in a single pore of such a medium. It is this pore model that we consider here with the former the subject of a future publication. We believe that this geometry has allowed us to perform a series of 'clean' experiments in order to be in a better position to unravel some of the basic effects under consideration for a miscible interface, and how they might be related to our more complete understanding of the boundary conditions in immiscible fluid displacement and instability.

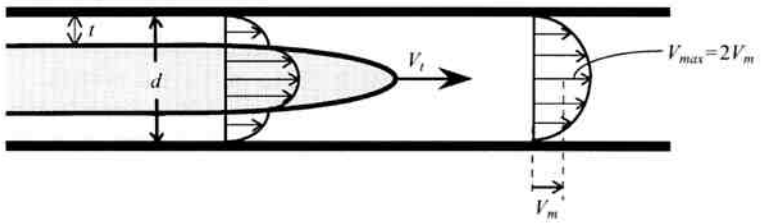


FIGURE 1. Schematic of miscible displacement in a capillary tube, showing the definition of $V_t$, $V_m$, $V_{max}$, $t$ and $d$, together with the velocity profiles within and upstream of the intruding finger.

In the immiscible case the seminal study of Taylor (1961) and the related numerical calculations of Reinelt & Saffman (1985) are the publications with which our results are to be compared. Taylor measured the amount of fluid displaced by injecting air into a horizontal capillary tube, initially filled by a viscous fluid, in order to calculate the mean velocity ($V_m$) of the Poiseulle flow ahead of the intruding finger. By simultaneously measuring the velocity of the tip ($V_t$) of the intruding air column he was able to calculate a quantity ($m$) that was related to the amount of displaced fluid that remained on the wall, i.e. $m = V_G/V_T = 1-(V_m/V_t)$, which, in turn, was related to the thickness ($t$) of the annular fluid layer left behind on the tube wall, i.e. $m = 1-(1-(2t/d))^2$; here $V_G$ is the volume of more-viscous fluid left on the tube wall over a length, $L$, $V_T$ is the total volume of the tube over the same length and $d$ is the tube diameter (figure 1). Note that as $2t/d \to 0$, $m \to 0$ and as $2t/d \to 1$, $m \to 1$, but the transformation from $2t/d$ to $m$ has had the effect of expanding the numerical range of $m$ for the values of $t$ of interest. The velocity profile in the tube was a 'double Poiseuille profile' connected through velocity and stress continuity conditions on the interface between the two fluids, as represented in figure 1. However, in Taylor's experiment the flow in the interior of the finger was dynamically unimportant because of the large viscosity ratios used. Ahead of the finger, the velocity profile was a Poiseuille profile with $V_m$ the means velocity and $V_{max} = 2V_m$ the maximum velocity at the centre of the tube.

Upon plotting $m$ *vs.* $Ca = V_t\mu_2/\sigma$ Taylor found a single curve for a number of fluids that increased from the origin as $Ca^{1/2}$, for small $Ca$, and that reached a value of 0.56 for moderately large $Ca$. Here $\mu_2$ is the dynamic viscosity of the displaced fluid and $\sigma$ the surface tension between it and the displacing air. In a later experiment Cox (1962) extended the range of $Ca$ and found an apparent asymptotic of 0.60 at large $Ca$. Numerical calculations by Reinelt & Saffman (1985), using the Stokes equations, agreed very closely with these experiments. Unfortunately no experiments have been run for viscosity ratios of the two fluids ($\mu_2/\mu_1$) other than the large values used by Taylor.

In the present work we have performed a version of Taylor's (1961) experiment in capillary tubes but using miscible fluids, glycerine and glycerine–water mixtures, in order to investigate a range of problems. The Atwood number $At = (\mu_2-\mu_1)/(\mu_2+\mu_1)$ was allowed to range over values from 0 to 1 so that, in general, the flow in the interior of the finger could no longer be ignored. The form of the $m$ *vs.* $Pe$ curve was of especial interest as was the effect of varying $At$. Here $Pe = V_{max}d/D$ is the Péclet number, and is the appropriate non-dimensional parameter to describe the flow, and $D$ is the 'average' diffusion coefficient between the two liquids (see §2.2). We have also measured the asymptotic value of $m$ for high $Pe$, as a function of $At$, and discuss the effects of gravity on the evolution of the instability. Further, we use this measurement

of the amount of fluid displaced, or alternatively the film thickness left on the tube wall, to determine an 'effective' surface tension and capillary number for the case $At = 1$, by directly comparing the present results with those of Taylor (1961).

The companion paper to this one (Chen & Meiburg 1996, hereafter referred to as Part 2), on the numerical calculation of miscible displacement in a capillary tube, should be considered as an integral part of the present paper. As will be seen, during the course of this work a great deal of interplay took place between the two efforts; the resulting interpretations rely heavily on this interaction.

## 2. Experimental arrangement and procedure

### 2.1. *Experiments on miscible displacements in capillary tubes*

A slightly modified version of Taylor's experimental set-up has been built (figure 2). The system consisted of a precision-bore glass tube with nominal inner diameter $d = 1, 2, 3$ or 4 mm, and a length of 1 m. The tube was mounted inside a square tube of 1 cm$^2$ section, and the region between the two tubes was filled with a glycerine–water mixture with the same refractive index as that of the glass, to allow an undistorted view of the flow inside the small cylindrical tube. Each end of the tube was connected to a constant-pressure tank, one filled with reagent grade glycerine, with a purity of 99.3% and a dynamic viscosity of $\mu_2 = 1020$ cP at 22.5 °C, and one filled with a glycerine–water mixture (with a concentration, by weight, of glycerine between 0 and 99.3%) so that $\mu_1$ varies between 1 and 1020 cP. The tube was first filled with glycerine ($\mu_2$), then, by suitable manipulation of the valves, a glycerine–water mixture ($\mu_1$) was forced into the tube displacing some of the glycerine. The displaced glycerine was collected in a receptacle placed on an electronic balance and weighted to an accuracy of 0.1 mg. From this measurement, and knowing the density of glycerine, we could deduce the volume of mixture injected in a given time. The mixture was coloured with blue food dye so that the interface could be observed through a low-powered microscope mounted onto an electronic ruler, thus giving the position of the interface to an accuracy of $\pm 0.5$ mm. Values of the diffusion coefficient of the dye in water were of the order of $10^{-7}$ cm$^2$ s$^{-1}$, which is comparable to that of the glycerine side of the interface (see §§2.2 figure 5), and therefore we anticipate that it will track this interface closely. When the dyed nose of the glycerine–water mixture had travelled a known distance, usually $L = 10$ cm, the amount of mixture that had entered the tube was measured, as outlined above, as was the time taken for the displacement. From this the average velocity, $V_t$, of the front was calculated as well as the average velocity, $V_m$, in the Poiseuille flow ahead of the finger. Owing to the experimental procedure adopted to generate the displacement, the velocity of the front was not constant during any one experiment. This was due to the fact that with a fixed pressure difference between the two ends of the tube the varying effective viscosity of the fluid in the tube gave rise to a slightly accelerating flow. For this reason we chose the distance $L$ small enough (10 cm) so that this change in velocity was small. Finally, as explained before, the diagnostic quantity $m = 1 - V_m/V_t$ was calculated. The experiment was then repeated for many values of the front velocity $V_t$ and Atwood number so that graphs of $m$ versus $Pe$ at constant initial $At$ could be constructed. In addition, similar experiments were performed in tubes of different diameters placed vertically, with either the glycerine or mixture as the lower fluid, or horizontally, in order to observe the effects of gravity on the form of the curves of $m$ *vs.* $Pe$ as well as on the interface shape.

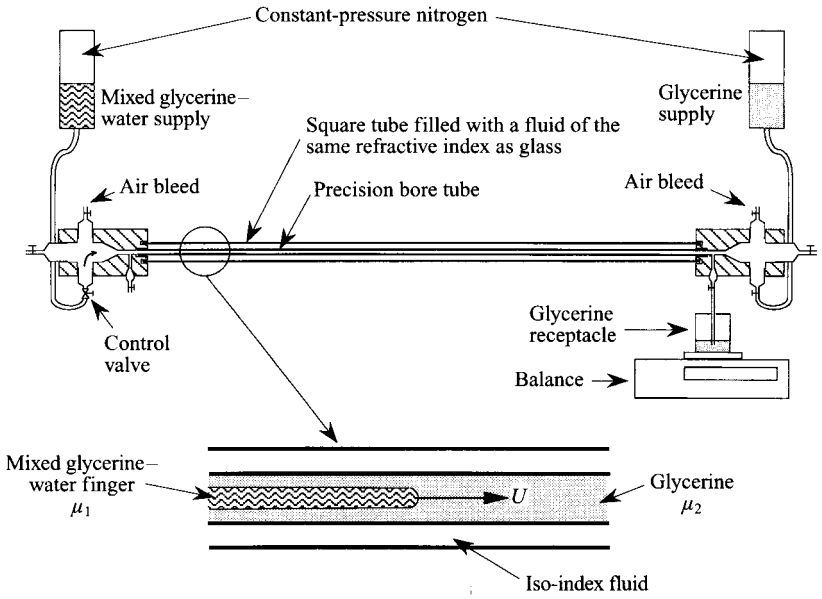


FIGURE 2. Apparatus. The capillary tube is enclosed in a square glass tube filled with refractive-index-matching fluid. The manifolds at each end are used to manipulate the glycerine and glycerine–water mixture as needed. The electronic balance is used to weight the amount of glycerine displaced by the intruding finger of mixture.

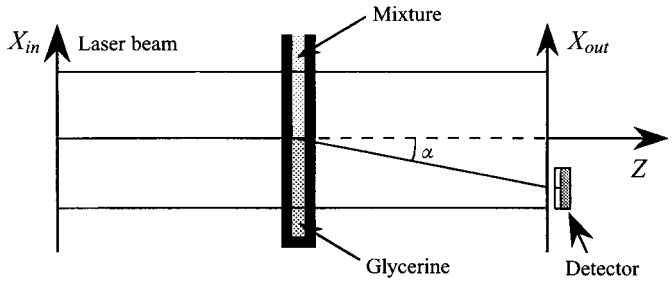


FIGURE 3. Sketch of the apparatus used to measure the diffusion coefficient between glycerine and a known glycerine–water mixture.

### 2.2. *Measurement of the diffusion coefficient, D*

In order to calculate the Péclet number the diffusion coefficient $D$ between glycerine and a known glycerine–water mixture was needed. Despite an exhaustive search of the literature we were unable to find values on which we felt we could rely. Therefore, it was decided to measure this coefficient in a separate experiment.

We assume that the one-dimensional equation of molecular diffusion describes the processes of interest, an assumption that is discussed in some detail in Part 2, and need not be repeated here. Here the 'average' diffusion coefficient, $D(C_g)$ (where $C_g$ is the percentage of glycerine by weight), for a number of fluid pairs was measured with the optical refraction method sketched in figure 3, while its local value, $D_L(C_g)$, in the dilute limit, was calculated from the results of the present experiments, using a modification of the technique used in Part 2 (§5). In this former method a focused laser beam was passed through a quartz cell that has been earlier partially filled with glycerine, on top of which was slowly added a similar amount of a known

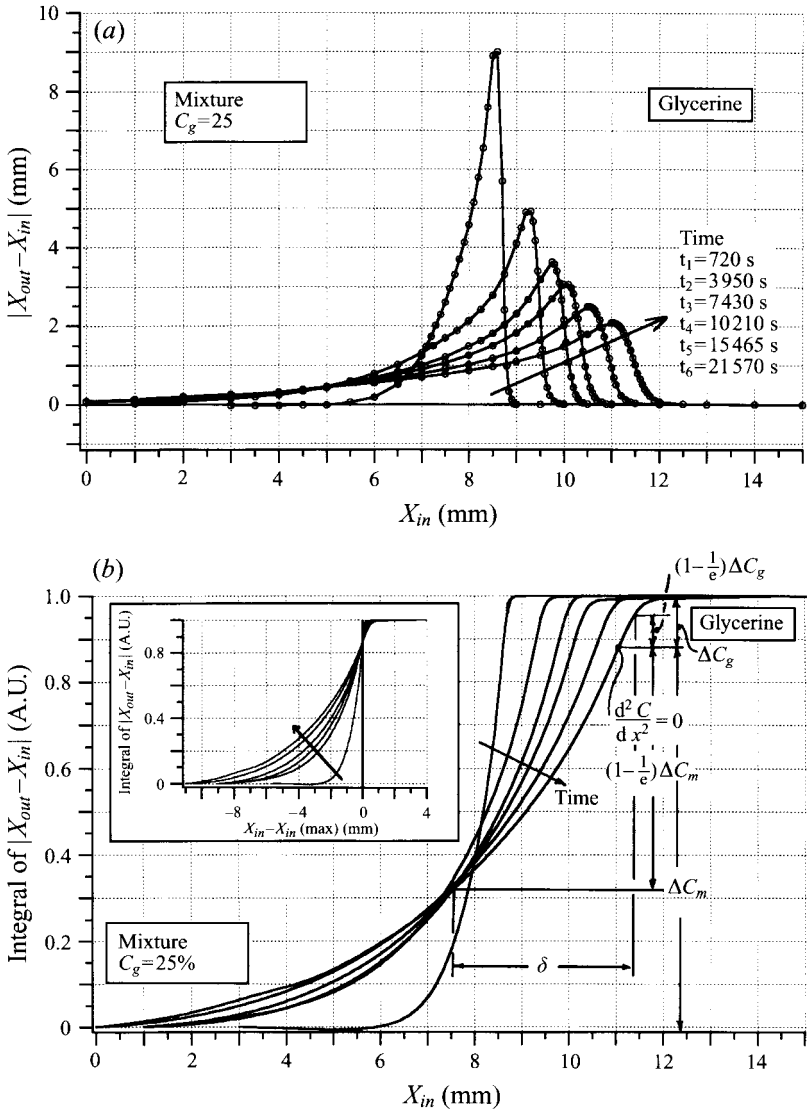


FIGURE 4. (*a*) Laser beam deflection as a function of its input or $x$-position, for the case where the diffusing mixture contains 25% glycerine by weight. This signal is proportional to the gradient of concentration ($dC_g/dx$). The times are shown on the figure. (*b*) The curves of $dC_g/dx$, in (*a*), have been integrated to show how $C_g$ varies with $x$, for the same times as (*a*). In (*a*) and (*b*) the movement of the maximum of $dC_g/dx$ is apparent, as is the very asymmetric form of the profiles. This latter point is emphasized in the inset figure which shows the profiles in a frame of reference fixed to the maximum of $dC_g/dx$. The thickness of the diffused layer ($\delta$) is defined as shown, i.e. to the $(1-1/e)$ locations on either side of the point of maximum slope.

glycerine–water mixture. The beam was bent vertically when it crossed a vertical gradient of concentration and this deviation was measured as a function of position within the interface with a light detector. The deflexion angle, $\alpha$, is given by the geometrical optical rule:

$$\alpha = \frac{n}{n_a}\int \frac{1}{n}\frac{\partial n}{\partial x}\,dz,$$

where $n$ (with respect to the value ($n_a$) for air) is the index of refraction of the fluid, and

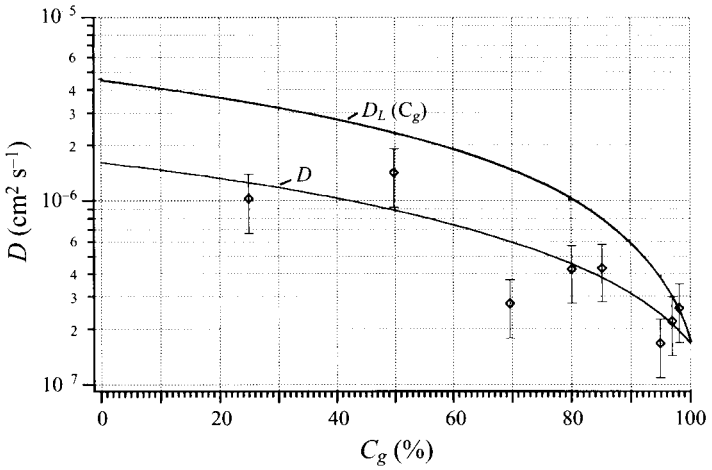


FIGURE 5. The 'average' diffusion coefficient between glycerine and a glycerine–water mixture, of a glycerine concentration by weight $C_g$. Also plotted are the values of the pointwise value of the diffusion coefficient, $D_L$, found by assuming that $D$ and $D_L$ must coincide at $C_g = 100\,\%$ and that $D_L$ is a linear function of $C_g$, as established in Part 2.

$z$ is in the direction of the undisturbed laser beam. Figure 4(*a*) represents the deviation of the laser beam versus position for different times after the formation of the interface. The maxima of the curves correspond to the position where the gradient of concentration is a maximum. An integration of these profiles gives curves (figure 4*b*) proportional to the concentration. Two points should be noted. (i) Unlike the profiles for a case with constant $D_L$, the curves of $C_g$ *vs.* $x$ show a movement of the point at which $\mathrm{d}^2C_g/\mathrm{d}x^2 = 0$ towards the glycerine side of the interface. (ii) The curves are very asymmetric with a broad variation in $C_g$ on the 'mixture' side and a sharp variation, almost a discontinuity, on the glycerine side. The suggestion that these effects are due to a large variation of $D_L$ with $C_g$, for the glycerine–water system used here, is borne out by the calculations in Part 2 and those presented below. However, for our present purposes, to calculate *Pe*, it is the single value of $D$ that is representative of the diffusion of the whole interface that is needed. From curves like those shown in figure 4(*b*) such an averaged or overall diffusion coefficient can be deduced, as function of the initial concentration of the mixture, by defining the width, $\delta$, to the $1-1/\mathrm{e}$ points of the profiles, on either side of the point with the maximum slope. Then, in analogy with the similar analysis of the symmetric error-function profile, $D = \delta^2/6.35t$, where $t$ is the time since the interface was formed. The resultant value of $D$ (figure 5) is then that *averaged for each particular mixture interdiffusing with pure glycerine*, and is given by the equation $D = 1.60 \times 10^{-6}\,(1 - 8.95 \times 10^{-3}\,C_g)$ cm$^2$ s$^{-1}$, with a correlation coefficient of 0.83. $D$ is not the same as the pointwise value, $D_L(C_g)$, calculated below, which is also plotted on the figure. Finally the Péclet number, *Pe*, is calculated with this averaged diffusion coefficient.

In order to calculate $D_L(C_g)$ note, first, that it and the average $D$ must be the same as a $C_g$ of 100 %, i.e. both represent the interdiffusion of glycerine plus an infinitesimal amount of water in pure glycerine. A value of $1.68 \times 10^{-7}$ cm$^2$ s$^{-1}$ is suggested by extrapolation of the present data. Secondly, from Part 2, §5, it was found that a linear variation of $D_L$ with $C_g$ is consistent with the measured velocity ($V_s$) of the point of maximum slope $(\mathrm{d}C_g/\mathrm{d}x)_{max}$. In what follows a value of $V_s/(\mathrm{d}C_g/\mathrm{d}x)_{max}$ of $4.25 \times 10^{-6}$ cm$^2$ s$^{-1}$ was used which, together with the value of $D$ at $C_g = 100\,\%$, gives the

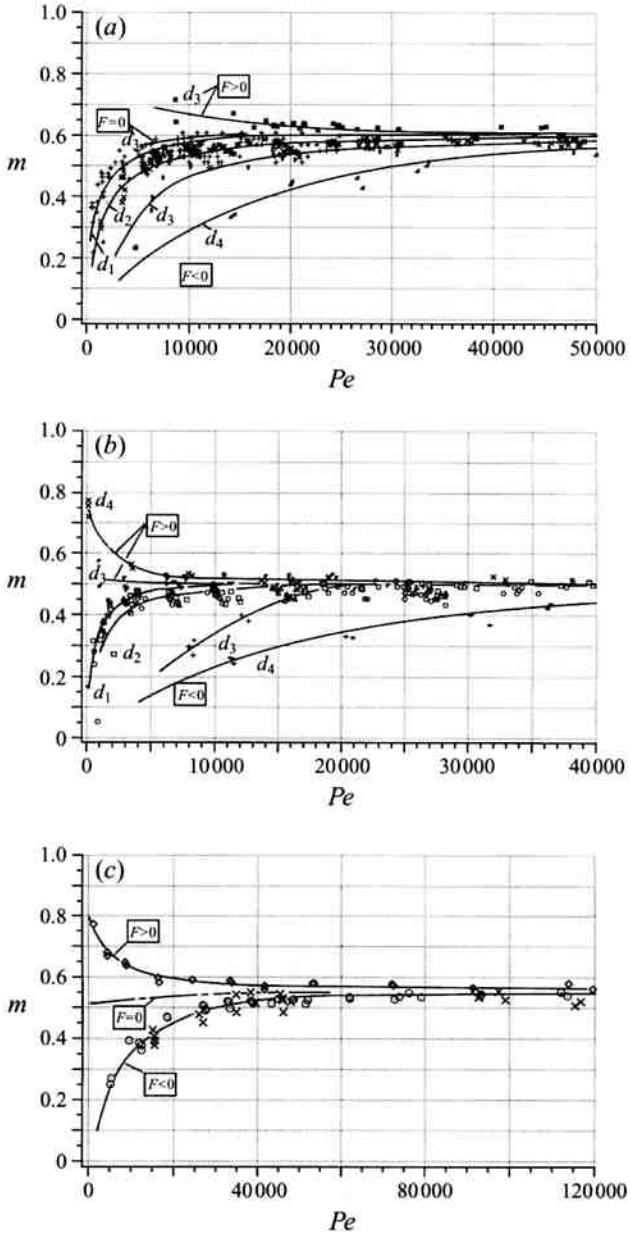


FIGURE 6. (*a*) The diagnostic quantity, $m$, versus Péclet number ($Pe$), for $At = 0.985$ and tubes of the various stated diameters set vertically, i.e. $d_1$ indicates a diameter of 1 mm etc. Here $F > 0$ for the case of glycerine above the mixture and $F < 0$ for the inverse. Here, as in all the graphs that follow, the lines were inserted by eye, based on considerable experience. Readers are invited to supply their own versions as needed. (*b*, *c*) The same as (*a*) but for $At = 0.43$ and 0.79 respectively. In (*c*) all curves are for a tube diameter of 3 mm and the interpolated curve for $F = 0$ is shown also (cf. figures 9(*a*) and 9(*b*) for $At = 0.785$ and 0.43 respectively).

curve shown on figure 5, the equation for which is $D_L = 4.43 \times 10^{-6}\,(1 - 9.62 \times 10^{-3}\,C_g)$ cm$^2$ s$^{-1}$. In the limit $C_g = 0$, $D_L(0)$ represents the interdiffusion of water and water plus an infinitesimal amount of glycerine, the dilute limit, while $D$ measures the interdiffusion

| Concentration of the mixture (%) | $At$ | $\mu_1$(cP) | $\rho_1$(g cm$^{-3}$) | $D$(cm$^2$ s$^{-1}$) |
|---|---|---|---|---|
| 100 | 0 | 1020 | 1.26 | $1.68 \times 10^{-7}$ |
| 94.41 | 0.43 | 352 | 1.25 | $2.48 \times 10^{-7}$ |
| 86.135 | 0.79 | 98.5 | 1.23 | $3.62 \times 10^{-7}$ |
| 55.69 | 0.985 | 7.5 | 1.13 | $8.02 \times 10^{-7}$ |
| 0 | 1 | 1 | 1 | $1.60 \times 10^{-6}$ |

TABLE 1. Some physical parameters for the experiments

of pure water with pure glycerine at an interface that covers the whole range of $C_g$ from 0 to 1 (100%). Values of $D_L(C_g)$ in this limit can be found in the literature but the results are widely scattered from $1.1 \times 10^{-5}$ to $3.5 \times 10^{-6}$ cm$^2$ s$^{-1}$. The present value of $4.43 \times 10^{-6}$ cm$^2$ s$^{-1}$ is that which results from an analysis of all of the experiments run here and is consistent with these previous measurements. Also the ratio of $D_L(0\%)/D_L(100\%)$, from figure 5, is 26.5, which is to be compared with a value of 40 found in Part 2, using a slightly different criterion to evaluate this quantity.

The reason for the difference between $D$ and $D_L$ is now clear from a study of the experimental data. The large variation of $D_L$ with $C_g$ makes the profile asymmetric, with very slow diffusion on the glycerine side of the interface. For example, at $C_g = 25\%$, $\delta$ is smaller by about a factor of 1.6 from the value it would have in the equivalent symmetric error-function profile, for diffusion in the dilute limit with constant $D_L$. Thus $\delta^2$ is smaller by a factor of around 2.6, a fact reflected in the smaller value of $D$ for the mixture/glycerine case.

One interesting consequence of this analysis is that in order to assure dynamic similarity between different systems not only must the geometry, $Pe$ and $At$ be the same but, also, the dimensionless variation of $\mu_1$ and $D_L(C_g)$ must have the same form.

During the experiments on the viscous displacement, to be described later, the 'fresh' mixture and glycerine are being convected into the region of the nose due to the flow pattern that is set-up in its neighbourhood (see §3). Because of this, it is reasonable to keep the same initial $D$ in the definition of $Pe$ for a given experiment, at least until diffusion at the lateral sides of the finger fills the tube with a mixture that has a radically different concentration from that set initially.

## 3. Results and discussion

A large number of experiments have been performed to measure $m$ as function of the different parameters: the Atwood number $At$, the tip velocity $V_t$, the diameter $d$ of the tubes, and the orientation of the tube, in order to take into account the effect of gravity. When the tube was oriented vertically clearly two possibilities existed: when the heavier fluid (glycerine, $\rho_2 = 1.26$ g cm$^{-3}$) was on top, gravity tended to destabilize the flow. Alternatively, when the lighter fluid (a mixture of glycerine–water, $\rho_1$ between 1 and 1.26 g cm$^{-3}$, depending on the concentration of glycerine) was on the top, gravity stabilized the flow. The relevant parameter is $F = g[(\rho_1 - \rho_2)/\rho_2]d^2/\nu_2 V_{max}$, which compares gravitational to viscous effects; cf. the rise of a bubble in a viscous fluid (Clift, Grace & Weber 1978, p. 33.). Here $\nu_2$ is the kinematic viscosity of the more-viscous fluid. As a result, $F$ is positive in the destabilized case (the heaviest fluids is on

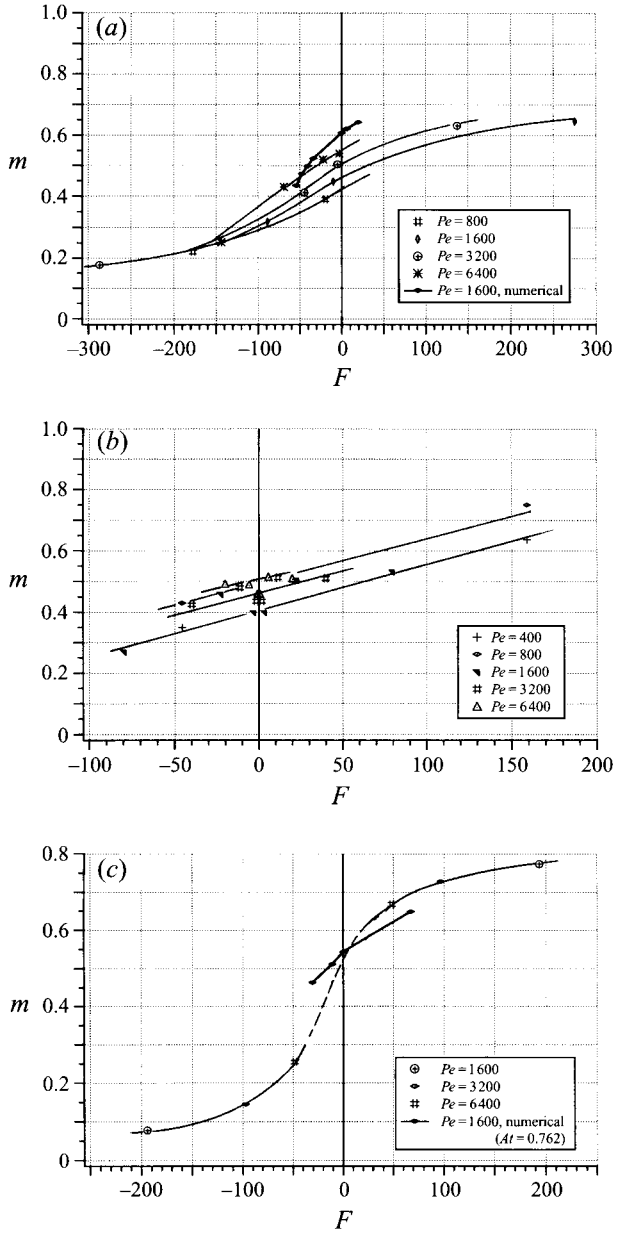


FIGURE 7. (*a*) A cross-plot of the data of figure 6(*a*) at $At = 0.985$ showing $m$ *vs.* $F$ for the various values of $Pe$ indicated on the figure. Data from Part 2 at $Pe = 1600$ are shown also. (*b*, *c*) The same as 7(*a*) but for $At = 0.43$ and 0.79 respectively. In (*c*) the dotted curve indicates that the interpolation is uncertain, since no intermediate points were measured.

the top), and negative in the stabilized case, while $F = 0$ when the tube is horizontal. As will be seen this does not mean that gravitational effects are negligible in this latter case, for the finger becomes distorted as it tries to rise within the narrow confines of the tube cross-section. We are only able to infer the symmetric finger behaviour, at $F = 0$, by interpolating within the results for the vertical intrusions for $F$ greater and less than zero. For the same two fluids a wide range of $F$ could be covered since

experiments were performed with tubes of 1, 2, 3 and 4 mm, diameter, as well as an extensive range of $V_t$.

Figure 6(*a*) gives the curves of the raw data of $m$ as a function of $Pe$ for tubes of different diameters, oriented vertically and horizontally, and for $At = 0.985$. In these experiments, the average velocity of the nose $V_t$ varied between 0.2 and 20 mm $s^{-1}$. It was extremely difficult to operate at slower velocities, typically values of $Pe$ below 1000, since diffusion had time to make the tip of the nose difficult to detect with the microscope (see later).

It is clear from these curves that gravity had a strong effect on the behaviour of the intruding finger. For large $Pe$ all the curves tend to the same value of $m$, which depends only on $At$, as we will show later. For small $Pe$, the behaviour of $m$ depends strongly on tube diameter and orientation, i.e. on $F$. When $F > 0$, $m$ increases as $Pe$ decreases which is opposite to the trend found for the case when $F < 0$, or even for the horizontal tube. Figures 6(*b*) and 6(*c*) give curves for values of $At$ of 0.43 and 0.79, while table 1 gives some physical values for these experiments.

In order to quantify the effect of the gravity, in figure 7(*a*) a cross-plot of $m$ as a function of $F$ for different $Pe$ and $At = 0.985$ is shown. Figures 7(*b*) and 7(*c*) give the equivalent curves for $At = 0.43$ and $At = 0.79$. For $At = 0.985$ and 0.79, the results obtained in Part 2, in the numerical simulations for the same values of $At$ and $Pe = 1600$, have been superimposed. The main points to note from all of these results is that while the calculations in Part 2 have reached the asymptotic value of $m$ at $Pe = 1600$, this limit is not reached in the experiments until much larger values, typically of order 10000 for the smallest tube diameter (1 mm). Also, in the experiments, because of the very small values of $D$ that result from the use of the glycerine–water system, it was not possible to operate in the Taylor dispersion limit discussed in Part 2, §4.2.

The difference of behaviour for the different signs of $F$ can be explained by reference to the sketches of figure 8. These represent the forces induced by gravity which change the profile of the finger and the thickness of the layer of displaced fluid left behind the advancing nose. In the gravitationally unstable case ($F > 0$), where the heavier fluid is placed on the top of the lighter one, the glycerine has a tendency to penetrate downwards along the wall of the tube, increasing the thickness of the glycerine layer around the finger, so that $m$ increases. In the opposite gravitationally stable case ($F < 0$), where the heavier fluid is placed under the lightest one, glycerine tends to leave the wall layer, thus decreasing the thickness of this layer, so that $m$ decreases also. In the horizontal case, gravity tends to move the main body of the lighter finger towards the upper part of the tube, even as the flow tried to enforce symmetry at the tip of the nose. In that case, the axisymmetry is affected, and its seems that the average amount $m$ of glycerine remaining on the wall is also modified for the larger tube diameters (see later). From the curves of figure 7, it is now possible to redraw, by interpolation or extrapolation, the evolution of $m$ as a function of $Pe$ for $F = 0$. Figure 9(*a*) gives such a result, for an $At$ of 0.785, where the measurements obtained with the tube of 1 mm of inner diameter have been superimposed. Note that in this comparison the results are not significantly different and within experimental error. Figure 9(*b*) gives the corresponding curve for an $At$ of 0.43, while the curve for $At = 0.79$ is included in figure 6(*c*).

In addition, for tubes of 3 and 4 mm inner diameter placed horizontally, a gravitational instability may appear which cuts the finger into two longitudinal parts, as shown in figure 10. This is a miscible version of the Rayleigh–Taylor instability. Kurowski & Misbah (1994) have studied the dispersion relation for the gravitational

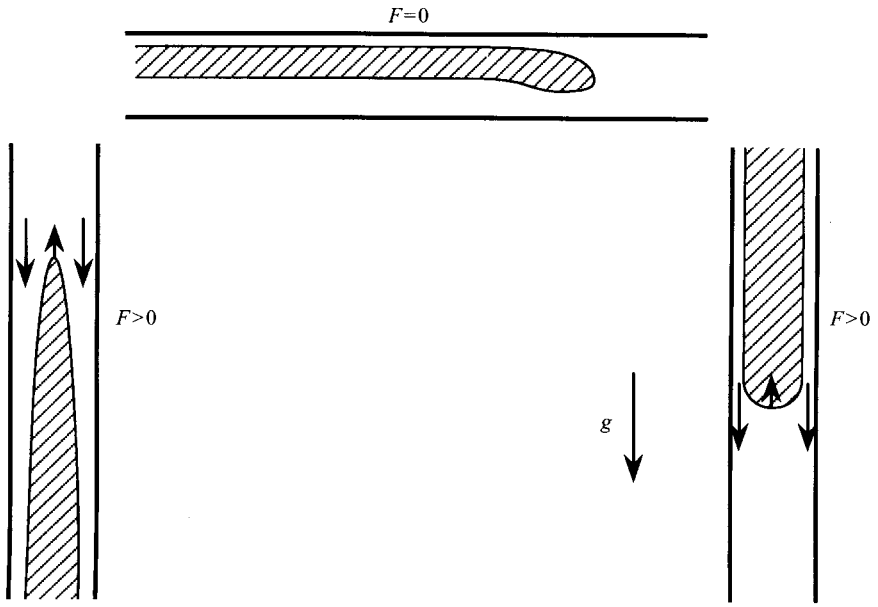


FIGURE 8. Sketches and photographs of the finger shapes for $F > 0$, $F < 0$ and $F = 0$ (a horizontal tube). The arrows on the sketches indicate the direction of gravity forces tending to the narrow the finger for $F > 0$ and widen it for $F < 0$. In all cases the hatched region represents the glycerine–water mixture.

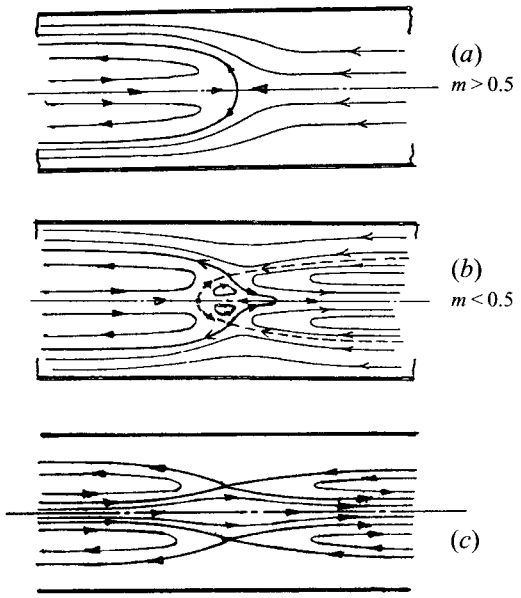


FIGURE 11. (*a*) A photograph and a sketch (modified from that in Taylor 1961) of the finger shape and steady streamlines, in a reference frame fixed to the fingertip, for $m > 0.5$. (*b*) The same as (*a*) but for $m < 0.5$. In the photographs shown here a thin spike grows continuously from the tip as a result of the recirculating flow field set-up in its neighbourhood. The hypothetical steady streamlines for this case are indicated in the sketch, which is a slightly modified version of that shown in Taylor (1961). In this instance, for simplicity, the unsteady growth of the spike is not taken into account in drawing the 'steady' streamlines. (*c*) A sketch of the unsteady streamlines associated with the growth of a spike at the nose of the finger, in a frame of reference moving with the nose not the tip of the spike! This is to be compared with similar sketches in Part 2, based on calculations.

FIGURE 8. For caption see facing page.

(*a*)

(*b*, *c*)

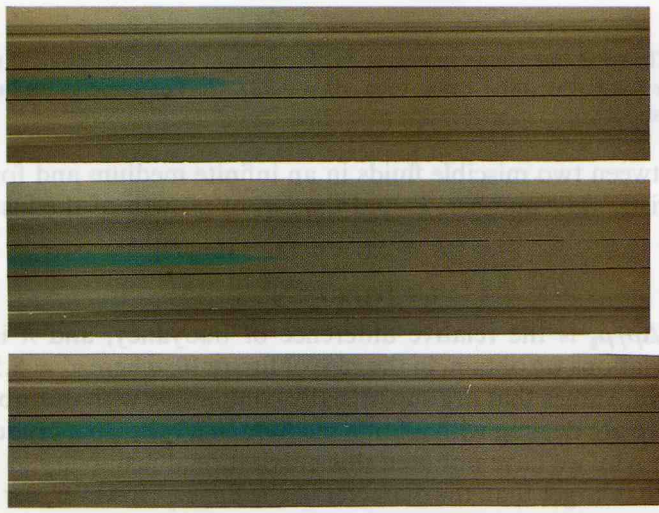

FIGURE 11. For caption see facing page.

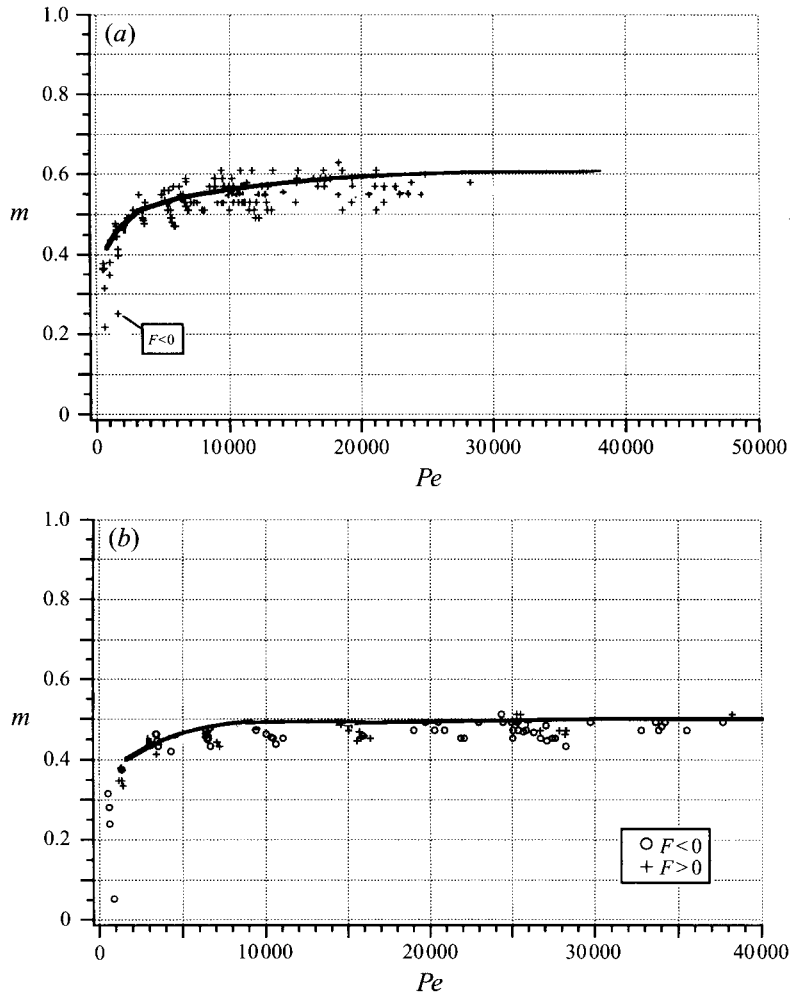


FIGURE 9. (*a*) The solid line shows $m$ versus $Pe$, for vertical tubes interpolated to $F = 0$. The crosses are for $m$ *vs.* $Pe$ for $F < 0$ and a 1 mm tube. $At = 0.985$. (*b*) The same as (*a*) but for $At = 0.43$. The sign of $F$ is as shown.

instability between two miscible fluids in an infinite medium and found equations for the characteristic wavenumber, $k$, and time, $t$, of growth of the instability given by

$$k = 2\pi/\lambda = [3g'/16\nu_2 D]^{1/3}$$

and

$$t = [\nu_2/g'D^{1/2}]^{2/3};$$

where $g' = g\Delta\rho/\rho_2$ is the relative difference of buoyancy, and $\lambda$ is the wavelength. Using these relations we obtain, in the case of figure 10, where $g' \approx 8.5$ cm s$^{-2}$, $t \approx 100$ s and $\lambda \approx 0.1$ cm, values that are superficially compatible with our observations despite the fact that we are dealing with a finite medium in a tube. In a crude way these results might explain why we have not seen this gravitational instability in the smaller tubes: the wavelength is larger than the diameter of the finger. However, for a larger difference in buoyancy, the theoretical wavelength is much smaller, but we have never observed the finger cut into more than two parts in such cases. Thus it seems that the wavelength is more likely to be controlled by the boundary conditions (the wall) and that the analysis for an infinite medium cannot give quantitatively reliable results in this case.

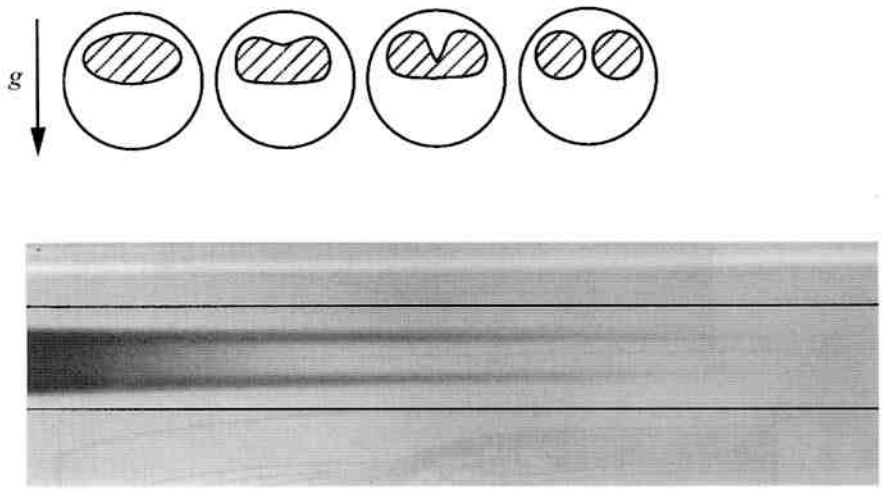


FIGURE 10. Finger splitting in a horizontal, 4 mm tube with the displacing fluid lighter than that displaced. The sketches indicate the cross-section of the instability at various locations along its length.

In order to interpret our results further note, following Taylor (1961), that there are two possible flow states: the first occurs when the velocity of the nose, $V_t$, is smaller than the velocity $V_{max}$, where $V_{max}$ is the velocity of the Poiseuille flow in the centre of the tube ahead of the finger; and the second when $V_t$ is larger than $V_{max}$. These two flows correspond respectively to $m < 0.5$ and $m > 0.5$. The transition from one state to the other occurs at a value of $Pe$ that depends on $At$ and $F$. When $m$ is larger than 0.5, the flow field is as shown in figure 11 (*a*) (see pp. 48 and 49), in a reference frame moving with the finger. There is only one stagnation point, at the tip of the nose. When $m$ is smaller than 0.5, Taylor (1961) proposed two interpretations for the steady streamlines: one with one stagnation point on the tip of the nose and a stagnation ring on the finger surface (figure 11 *b*), and another with two stagnation points on the axis. We have found in our experiments with miscible displacements that when $m < 0.5$ a very thin finger, or 'spike,' emerged from the tip of the principal finger and moved through the displaced fluid. In the sequence of photographs of figure 11 (*b*), we show the growth of this 'spike' starting from the tip of the main finger. It could become quite long (a few cm) provided $m < 0.5$. The absence of a large surface tension in the present experiment explains why the finger can form in this case and not in the immiscible case. In the latter the large surface tension does not allow such a small radius of curvature at the nose of the 'spike' in the strain field generated by the tip motion. Its existence can now be attributed to the recirculating flow ahead the finger, as shown in figure 11 (*b*) for the equivalent steady situation and in figure 11 (*c*) for an unsteady flow with a growing spike. On the other hand it is not compatible with the other proposition presented by Taylor. This observation suggests that for $m < 0.5$ the solution with a stagnation ring, off the axis of symmetry, is the correct one not only in the miscible case, but also in the immiscible case since the miscibility only changes the streamlines near the axis, with a growing spike in the first case and a stagnation point in the second. Note that the growth of this 'needle' was not taken into account in the measurement of the timed change in the length of the finger used to calculate $V_t$. This in turn means that the small amount of fluid represented by the growth of the needle was not taken into account when calculating $V_t$. From photographic sequences like figure 11 (*b*) we estimate that

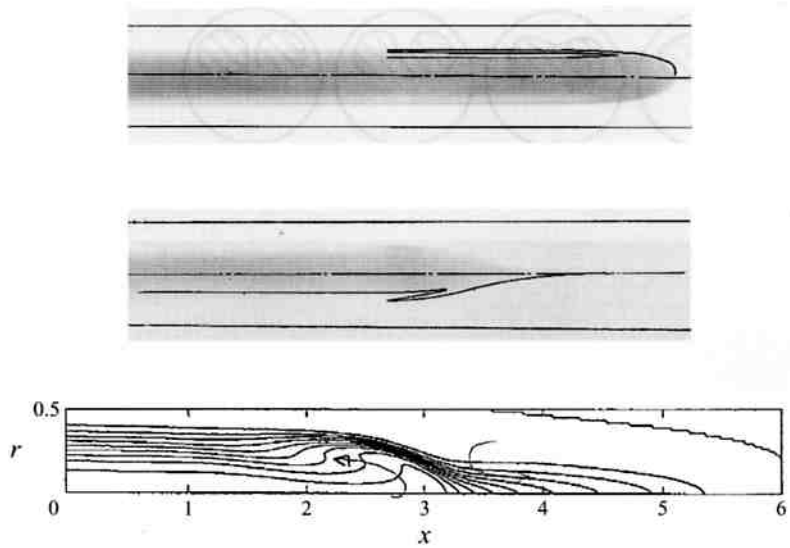


FIGURE 12. Partially enhanced photographs of the finger tip, indicating the reversed flow that exists at the nose, under some circumstances when $m < 0.5$. The line drawing is from Part 2 for a situation similar to that shown in the lower photograph.

the increase in 'needle' volume, over a given time interval, is less than 3% of the increase in volume of the primary finger.

In this same flow regime we have observed, also, recirculation in the nose of the finger. Figure 12 shows photographs where this can be seen. This deformation, which has the form of a 'plume' is quite similar to what has been obtained in Part 2 in their numerical simulation, which is also reproduced in figure 12 (figure 16 of Part 2). This recirculation is one reason why the interface at the nose could be very thin, and not diffuse, even for low $Pe$ ($\approx 1000$). At these low values of $Pe$ diffusion that occurs on the sides of the finger may perturb the 'purity' of the mixture coming into the nose. To estimate this effect note that diffusion mixes the fluids over a thickness $\delta_1 \approx (\nu L/V_{max})^{1/2}$, where $L$ is a representative length over which we assume the contamination of the initial mixture becomes important. Assuming that this contamination takes place when $\delta_1 \approx d/2$ leads to the requirement that $L/d \approx Pe/4$. That is the length of the finger that can usefully be used in any one experiment, before contamination of the intruding fluid becomes a critical issue, is limited at the lower tip velocities, being about a quarter of the length of the tube in the most extreme case, i.e. at the lowest $Pe \approx 100$ and in a 1 mm inner diameter tube.

For very large $Pe$, $m$ tends to an asymptotic value $m_{max}$ that depends only on the Atwood number, and not on the diameter of the tube nor on its orientation. Figure 13 shows this dependence. We observe that for $At < 0.5$, $m_{max} \approx 0.5$. For higher $At$, $m_{max}$ increases to a value of 0.61. Unfortunately, we could not find any extensive experimental results for the immiscible case in order to compare with these asymptotic values, except for the one case (Taylor 1961) discussed later. Nevertheless, this evolution is very similar to that obtained in the numerical simulations in Part 2 and which are presented on the same figure. Templeton (1953) and Goldsmith & Mason (1963) studied the immiscible liquid–liquid displacement of bubbles in small tubes, and observed that the thickness of the residual film increased as the Atwood number decreased for a given $Ca$, which is in an opposite sense to that found in the miscible case. This is a surprising observation since we would expect the same asymptotic value

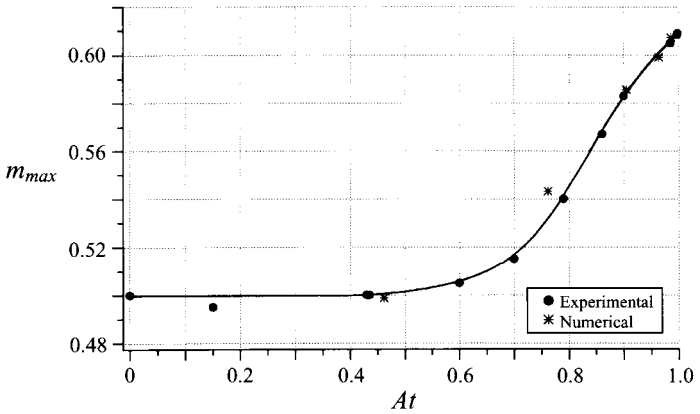


FIGURE 13. The asymptotic value of $m$ (i.e. $m_{max}$) at large $Pe$, as a function of $At$. The corresponding points from (Part 2) are shown also.

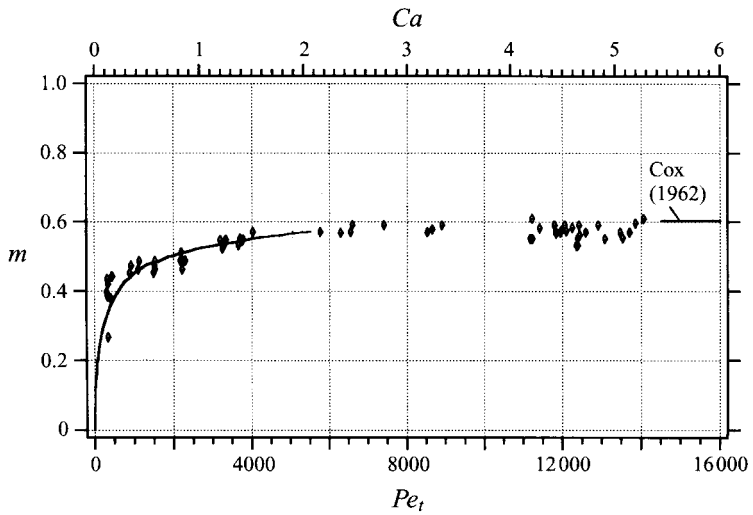


FIGURE 14. A comparison between $m$ *vs.* $Pe_t$, for miscible flow in a 1 mm diameter tube and $F \approx 0$ (diamond symbols) and Taylor's (1961) result from $m$ *vs.* $Ca$ for immiscible fluids (curve), both for $At = 1$. The abscissae have been scaled to bring about a coincidence between the two sets of results in their range of overlap.

of $m_{max}$ in both cases based on the following argument. Infinite capillary number can be interpreted as immiscible flow with zero surface tension. In the same way, infinite Péclet number can be interpreted as a miscible flow with zero diffusion. In other words, it is possible to formally identify the interface between two immiscible fluids without surface tension with that between two miscible fluids without molecular diffusion. In that sense, the asymptotic value $m_{max}$ should be the same in both the immiscible and miscible cases, although, as pointed out by a referee, it is possible that the limiting cases may, in fact, be singular. However, it is not clear why the quoted studies found different results from the present experiments; this is a problem to be left for a future study.

Finally, Taylor's (1961) paper is the only one from which we can get an extensive immiscible curve of $m$ versus $Ca$. Thus, for $At \approx 1$, the immiscible and miscible data can be compared in order to determine, formally, an 'effective' surface tension, $\sigma_{eff}$, between two miscible fluids such as water and glycerine. The maximum value of $m$ in

Taylor's experiment was $m_{max} = 0.56$ while we find $m_{max} = 0.61$ in the miscible case. This difference can be rationalized by the observation that Taylor, apparently, did not reach the asymptotic value but stopped at too small a capillary number. In later experiments Cox (1962) found $m_{max} = 0.60$, a value that is very close to our result. Figure 14 shows the two curves (miscible and immiscible) superimposed on the same graph. Here $Pe_t = V_t d/D = 8000$ is equivalent to $Ca = \mu V_t/\sigma = 3$, so that we obtain a value of the 'effective' surface tension of $\sigma_{eff} = 2670\ \mu D/d \approx 0.43$ dyn cm$^{-1}$, for the fluids used here in a 1 mm diameter tube. As a comparison, this value is about 0.7% of the surface tension between glycerine and air (i.e. $\sigma_{gly-air} \approx 62$ dyn cm$^{-1}$), and is of the same order as the value of 0.58 dyn cm$^{-1}$ found by Petitjeans (1996), for the water–glycerine system, using the 'static' 'rotating-drop' method.

## 4. Conclusions

This experimental work is complemented by a numerical study by Chen & Meiburg (1996) presented as Part 2 of this submission. As a result of the very small values of $D_L$ that exist in the fluid system used here, there is only one regime where comparisons can usefully be made. This corresponds to high $Pe$ ($> 10^3$). The results are in very good agreement with each other in some respects and not in others. In particular, the evolution of the asymptotic value of $m_{max}$ for high $Pe$ as a function of the Atwood number is found to be very similar in both studies. The interface remains very sharp in both cases, mainly because of the convective motion that occurs on both sides of the nose of the finger and which brings fresh fluid into that region (see Part 2, §4.1.1). However, the magnitude of the transition Péclet number to this asymptotic state is quite different in the two studies. Also the variation of $m$ with smaller values of $Pe$ is not the same in the experiments as in the calculations. These differences must be due, to a large extent, to the assumption used in Part 2 of a constant diffusion coefficient, while in the experiment $D_L(C_g)$ varies by a factor of order 26.5, for the larger values of $At$ (see figure 5). Also the variation of viscosity with concentration in the present experimental system is best represented by a double exponential function of concentration above $C_g \approx 20\%$ and a single exponential below, while the numerical calculations use a single exponential over the whole range of $C_g$. It is clear that both diffusion of species and vorticity, acting at the tip of the finger, are absolutely critical in determining the shape of the nose and hence the overall shape of the finger. At this location, small differences in the variation of the two diffusion coefficients with concentration almost certainly have important effects, with that of species diffusion probably the most critical.

For values of $Pe < 1000$, where in Part 2 the existence of a regime of Taylor dispersion is predicted, it has not been possible to obtain any meaningful experimental results. This was due, mainly, to the inability to define accurately an interface between the two fluids. This inability suggests that, in fact, the diffusion-dominated regime had been reached, thus confirming the suggestion in Part 2, not by quantitative measurement but by a qualitative observation.

The important effect that the gravitational force may have, even at moderate to high values of $Pe$, has been revealed. Nevertheless, it has been found possible to interpolate the amount of fluid remaining on the wall, $m$, as a function of the Péclet number, to the zero-gravity case, for a vertical tube. As noted previously the numerical simulations give smaller values of $m$ at high $At$ ($At = 0.985$, figure 7$a$), although the agreement is better for lower values ($At = 0.79$, figure 7$c$). An examination of figures 7($a$) and 7($b$) makes it clear that the curves have not reached the asymptotic of $m$ at $Pe = 1600$, for

these values of $At$ and for this experimental system, that encompasses a large variation of $D_L$ within the interface region. On the other hand the calculations in Part 2, that use a constant $D_L$, have reached their final value. Closer agreement for $At = 0.79$ may actually be fortuitous since the experimental data are not extensive enough to define the curve for $F = 0$ accurately (note that the curve is shown dashed in figure 7*c* to denote this fact). As a result one should expect the values to coincide only at larger experimental values of $Pe$.

It has been possible to obtain an 'effective' surface tension between water and glycerine by comparing the immiscible (Taylor 1961) and the present, miscible experiments for $At = 1$. The value obtained, $\sigma_{eff} \approx 0.43$ dyn cm$^{-1}$ for a 1 mm diameter tube, is of the same order of the value of 0.58 dyne cm$^{-1}$ found by Petitjeans (1996) in a direct measurement using the 'rotating-drop' method. Both are significantly larger than values ($O(10^{-4})$ dyne cm$^{-1}$) calculated by Davis (1988), for example, for a case where $D_L$ was a constant.

The support, through Grant Number DE-FG03-93ER14346, of the Basic Sciences Division of the Department of Energy is gratefully acknowledged as is that of the Petroleum Research Fund of the American Chemical Society, through Grant PRF # 26311-AC. The support through a NATO Collaborative Research Grant is also gratefully acknowledged. We thank, also, our co-workers, Professor E. Meiburg and Mr C.-Y. Chen, for their fundamental contributions to the interpretation of the experiments presented here.

## REFERENCES

Bensimon, D., Kadanoff, L. P., Liang, S., Shraiman, B. I. & Tang, C. 1986 Viscous flows in two dimensions. *Rev. Mod. Phys.* **58**, 977.

Brady, J. F. & Koch, D. L. 1988 Dispersion in porous media. In *Disorder and Mixings* (ed. E. Guyon *et al.*). NATO ASI Series E, Academic.

Chen, C.-H. & Meiburg, E. 1996 Miscible displacements in a capillary tube. Part 2. Numerical simulations. *J. Fluid Mech.* **326**, 57 (referred to herein as Part 2).

Chouke, R. L., Meurs, P. van & Pol, C. van der 1959 The instability of slow, immiscible, viscous liquid-liquid displacements in permeable media. *Trans. AIME* **216**, 188.

Clift, R., Grace, J. R. & Weber, M. E. 1978 *Bubbles, Drops and Particles*. Academic.

Cox, B. G. 1962 On driving a viscous fluid out of a tube. *J. Fluid Mech.* **14**, 81.

Davis, H. T. 1988 A theory of tension at a miscible displacement front. In *Numerical Simulation in Oil Recovery* (ed. M. Wheeler). Springer.

Goldsmith, H. L. & Mason, S. G. 1963 The flow of suspensions through tubes, Part II. Single large bubbles. *J. Colloid Sci.* **18**, 237.

Homsy, G. M. 1987 Viscous fingering in porous media. *Ann. Rev. Fluid Mech.* **19**, 271.

Hu, H. H. & Joseph, D. D. 1991 Interfacial tension between miscible liquids. Preprint of the Dept, of Aero. Engng., University of Minnesota.

Joseph, D. D. 1990 Fluid dynamics of two miscible liquids with diffusion and gradient stress. *Eur. J. Mech.* B/ *Fluids* **9**, 565.

Korteweg, D. J. 1901 Sur la forme que prennant les equation du movement des fluides si l'on tient compte des forces capillaires causees par des variations de densite. *Arch. Neerl. Sci. Ex. Nat.* (ii) **6**, 1.

Kurowski, P. & Misbah, C. 1994 A non-standard effect of diffusion on a fictitious front between miscible fluids. *Eur. Phys. Letts.* **29**, 309.

Maxworthy, T. 1989 Experimental study of instability in a Hele-Shaw cell. *Phys. Rev.* A **39**, 3863.

Meiburg, E. & Homsy, G. M. 1988 Nonlinear, unstable, viscous fingers in Hele-Shaw flows. Part 2: Numerical simulations *Phys. Fluids* **31**, 429.

PETITJEANS, P. 1996 Une tension de surface pour les fluides miscibles. *C. R. Acad. Sci. Paris* serie IIb **322**, 673.

REINELT, D. A. & SAFFMAN, P. G. 1985 The penetration of a finger into a viscous fluid in a channel and tube. *SIAM J. Sci. Statist. Comput.* **6**, 582.

SAFFMAN, P. G. 1986 Viscous fingering in Hele-Shaw cells. *J. Fluid Mech.* **173**, 73.

SAFFMAN, P. G. & TAYLOR, G. I. 1958 The penetration of a finger into a porous medium in a Hele-Shaw cell containing a more viscous liquid. *Proc. Roy. Soc. Lond.* A **245**, 312.

TAN, C. T. & HOMSY, G. M. 1986 Stability of miscible displacements in porous media: rectilinear flow. *Phys. Fluids* **29**, 3549.

TAYLOR, G. I. 1961 Deposition of a viscous fluid on the wall of a tube. *J. Fluid Mech.* **10**, 161.

TEMPLETON, C. C. 1953 A study of displacements in microscopic capillaries. *Petrol. Trans. AIME* **33**, 162.

YORTSOS, Y. C. & ZEYBEK, M. 1988 Dispersion driven instability in miscible displacement in porous media. *Phys. Fluids* **31**, 3511.

ZIMMERMAN, W. & HOMSY, G. M. 1991 Nonlinear viscous fingering in miscible displacement with anisotropic dispersion. *Phys. Fluids* A **3**, 1859.